Inverse analysis for calibration of FRP – concrete interface law

M. Savoia, B. Ferracuti & L. Vincenzi
DISTART- Structural Engineering, University of Bologna, Bologna, Italy

ABSTRACT: Inverse analysis technique is used to derive a non linear mode II interface law for Fiber Reinforced Polymer (FRP) – concrete bonding starting from experimental data. The proposed interface law is based on a fractional formula and includes non linear compliance contributions of adhesive and concrete cover at high shear stresses. It depends on three parameters (maximum shear stress, corresponding slip and an exponent), which are calibrated from experimental results on delamination tests. Values of maximum loads for different bonding lengths and strains profiles along FRP plates are used. Parameter identification is performed by inverse analysis using a Direct Search technique. Considerations on well-posedness of inverse problem adopting different cost functions are given. After parameter identification, numerical results obtained with the proposed interface law are found to be in very good agreement with experimental results.

1 INTRODUCTION

It is well known that failure modes due to FRP delamination may significantly reduce the theoretical bearing capacities of FRP-strengthened R/C beams. A complete knowledge of bond-slip law in terms of fracture energy, peak point and initial stiffness, is fundamental to correctly design FRP retrofitting. First, for sufficiently long bonded lengths, ultimate failure load due to delamination mainly depends on fracture energy of mode II interface law. Moreover, evaluation of effectiveness of strengthening under service loadings requires to calculate stress concentrations close to transverse cracks in concrete and verify it is lower than peak shear stress (Teng et al. 2003, CNR Committee 2006). In the linear range, stress concentration is governed by initial stiffness of the interface, where compliances of both adhesive and external cover of concrete must be taken into account.

In Teng & Smith (2002), some recently proposed interface laws are reviewed. The most common interface law is based on a bilinear shear stress – slip relation, with peak shear stress defined from Mohr-Coulomb criterion for concrete and corresponding slip arbitrarily assumed, and final slip of softening branch defined in order to attain a given value of fracture energy of the law (about 0.15-0.2 mm). Comparison with more sophisticated laws (Ferracuti et al. 2006) showed that this relation is very rough for several reasons: first of all, peak shear stress cannot be obtained from concrete properties only,

depending also on surface preparation before bonding and the adopted adhesive; moreover, slope of linear softening branch has not a physical meaning. As a result, delamination force for short bonded lengths is strongly overpredicted.

A power fractional FRP – concrete interface law has been proposed by Ferracuti et al. (2007), whose parameters (peak shear stress, corresponding slip and an exponent) are calibrated by post-processing experimental data: from equilibrium and compatibility considerations, average shear stress and slip data are computed, and a least-square procedure is adopted to determine the parameters. This study clearly shows that, from the experimental point of view, evaluation of maximum delamination force (global data) or applied force – plate displacement curves only is not sufficient to provide data to define a shear stress – slip interface law. Very accurate tests with measure of strains (local data) along the FRP plate are also needed.

In the present paper, a more complete inverse analysis procedure is used to calibrate the parameters of a non linear constitutive law for FRP – concrete interface. The previously quoted interface law and a bond – slip model recently proposed by the authors (Ferracuti et al. 2006), are adopted.

Inverse analysis technique is applied to a set of experimental results by Mazzotti et al. (2007) on FRP – concrete delamination. Experimental results have been obtained in terms of strains on FRP plate at different values of applied force and delamination forces for different bonding lengths.
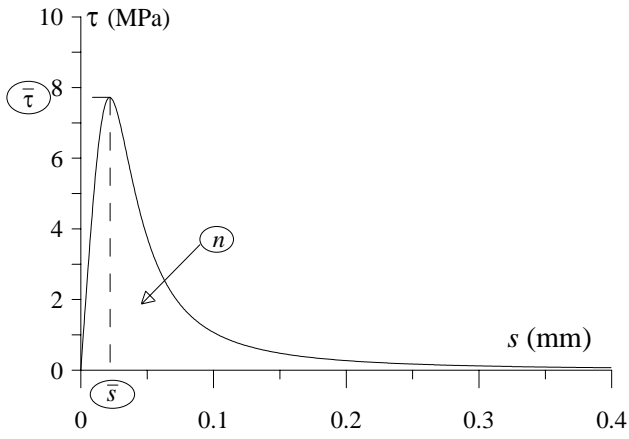
Figure 1. The proposed FRP – concrete interface law (see Equation 1), for $n = 3.008$, $\overline{\tau} = 7.72$ MPa, $\overline{s} = 0.0218$ mm.
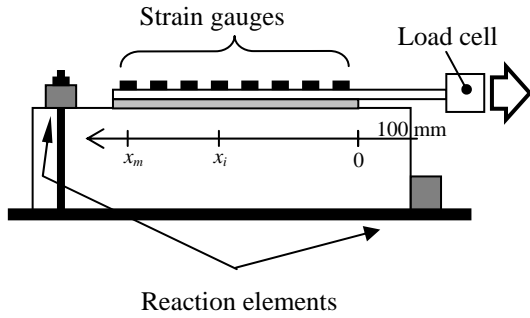

Figure 2. Pull-pull setup for FRP-delamination test (from Mazzotti et al. (2007)).

Identification method based on genetic algorithms (Storn & Price 1997) is used to perform inverse analysis. The adopted method (Differential Evolution algorithm) is a direct search approach, which is able to avoid convergence on local minima of cost function. In the present problem, the cost function is a weighted sum of errors on prediction of strains along the FRP plate and delamination forces. Considerations on well-posedness of inverse problem are drawn. It is shown that, as already underlined in inverse problems in very different frameworks (see Iacono et al. 2006 and Slowik et al. 2006 for identification of softening law of concrete in tension or Savoia & Vincenzi 2005 for identification of mechanical properties of structures from dynamic tests), well-posedness is achieved only if both global data (e.g. load – deflection curves) and local data (strains along FRP plate) are considered in cost function.

Finally, parameters obtained from inverse analyses have been used to simulate experimental tests and numerical results are found in very good agreement with experimental results.

2 FRP-CONCRETE INTERFACE LAW

The definition of a mode II interface FRP - concrete law is a difficult task for several reasons. From the experimental point of view, tests where force – displacement curves only are determined do not provide for sufficient data to define a local interface law. Measures of strains along FRP plate are also required. On the other hand, transmission length of local stresses at the interface level is very small, less than 80-100 mm from bonding extremity, and several strain gages must be placed within that length.

Moreover, interface law and numerical model are strictly interconnected: kinematic variables the interface law is referred to depend on the features of the adopted model. For instance, in the present model (see Section 4), slip is referred to average displacement of concrete cross-section and, consequently, interface compliance must take shearing deformation of both adhesive and external cover of concrete into account, also at high shear stresses. At load levels typical of service loadings (about 50 per cent of maximum load), maximum slip may already exceed that corresponding to peak shear stress. Softening branch is also very important, since fracture energy of interface law and, consequently, maximum transmissible load strongly depend on it.

Following Ferracuti et al. (2007), the adopted interface law is a power fractional law (see Figure 1):

$$\tau = \overline{\tau}\, \frac{s_p}{\overline{s}}\, \frac{n}{(n-1) + (s_p/\overline{s})^n}, \qquad (1)$$

where τ, s_p are FRP-concrete shear stress and slip. Moreover, $\overline{\tau}$, $\overline{s}$ indicate maximum shear stress and corresponding slip, whereas $n > 2$ is a parameter mainly governing the softening branch. Equation 1 is depicted in Figure 1, adopting values of parameters ($\overline{\tau}$, $\overline{s}$, n) obtained in numerical application reported in Section 6.

3 CALIBRATION OF INTERFACE LAW BY INVERSE ANALYSIS

3.1 Experimental test by Mazzotti et al. (2007)

In order to calibrate an interface law, four pull-pull tests from the experimental campaign by Mazzotti et al. (2007) are considered in the present study (Figure 2). Four different bonded lengths BL (50, 100, 200 and 400 mm) were tested, by gluing CFRP plates (plate width $b_p = 80$ mm, thickness $h_p = 1.2$ mm) to concrete blocks (150×200×600 mm).

Data obtained from experimental tests are maximum transmissible forces F for different bonding lengths and axial strains ε along the FRP plate for different levels of applied load.

3.2 Global data: maximum force

As well known, increasing the length of the anchorage, transmissible force increases asymptotically up to a maximum value, depending on fracture energy of interface law and mechanical/geometrical proper-

ties of the plate. Maximum transmissible force by an anchorage of infinite length is defined as:

$$F_{\max} = b_p \int_0^\infty \tau(x) \cdot \mathrm{d}x, \tag{2}$$

with b_p = plate width, and the following relation holds between $F_{\max}$ and fracture energy of interface law G_f (see Ferracuti et al. 2006):

$$F_{\max} = b_p \sqrt{2E_p h_p G_f} . \tag{3}$$

where h_p, E_p stand for thickness and elastic modulus of FRP plate. Equation 3 shows that a correct estimate of fracture energy is fundamental for the definition of interface law, because only in this case the value of maximum transmissible load can be accurately predicted.

For the proposed interface law, fracture energy can be expressed in closed form as a function of governing parameters ($\overline{\tau}$, $\overline{s}$, n):

$$G_f = \int_0^{+\infty} \tau(s_p)\,\mathrm{d}s_p = g_f(n)\,\overline{\tau}\,\overline{s} \tag{4}$$

where g_f is given by:

$$g_f(n) = \pi \left(\frac{1}{n-1} \right)^{1-\frac{2}{n}} \frac{1}{\sin(2\pi/n)} \tag{5}$$

Equation 5 confirms that Equation 1 requires $n > 2$, otherwise the fracture energy is not a positive and finite quantity.

3.3 Local data: axial strain along FRP plate

As shown in Figure 3b, distribution of strains along the plate for low values of applied load is governed by the initial stiffness of interface law. Initial stiffness of the adopted interface law can be written as a function of three unknown parameters ($\overline{\tau}$, $\overline{s}$, n) as:

$$k_p = \lim_{s_p \to 0} \frac{\tau(s_p)}{s_p} = \frac{\overline{\tau}}{\overline{s}} \frac{n}{n-1} \tag{6}$$

On the contrary, for high values of applied load, maximum slope of strain profile along the plate is governed by the maximum shear stress $\overline{\tau}$ (see Figure 3b), as shown by the following equilibrium equation:

$$\overline{\tau} = \frac{A_p}{b_p} \left(\frac{\mathrm{d}\sigma_p}{\mathrm{d}x} \right)_{\max} = \frac{E_p A_p}{b_p} \left(\frac{\mathrm{d}\varepsilon}{\mathrm{d}x} \right)_{\max} \tag{7}$$

where A_p, E_p stand for area and elastic modulus of FRP plate, whereas σ_p, ε are axial stress and strain of FRP.

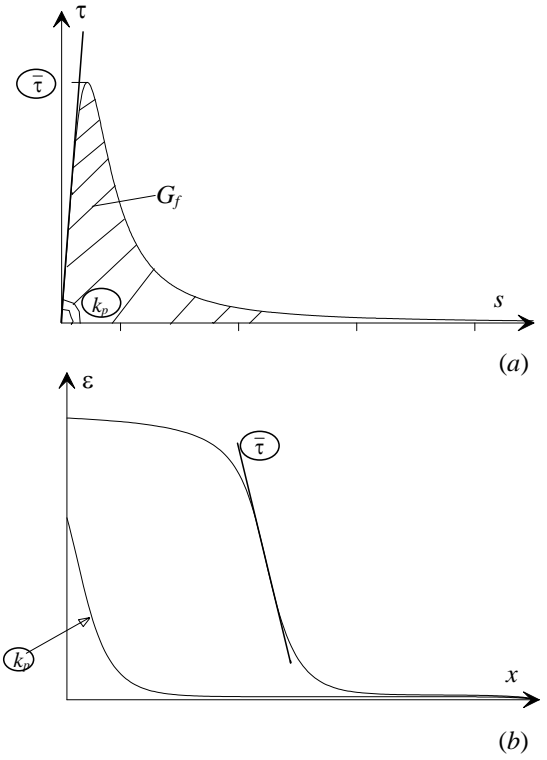Therefore, if experimental values of maximum forces at delamination only are adopted for parame-

Figure 3. (a) The proposed interface law and (b) a typical distribution of strains along the plate before and after the onset of delamination: k_p = initial stiffness, $\overline{\tau}$ = peak shear stress, G_f = fracture energy of interface law.

ter estimation, ill-posedness of identification problem can be expected. In fact, except for the case of very short bonded lengths, maximum transmissible load by an anchorage depends on fracture energy of interface law only, as confirmed by Equation 3. Three unknown parameters cannot be identified using one information only. On the contrary, if values of strains along FRP plate are also used, two additional information are introduced (initial stiffness and peak shear stress), and a well-posed identification problem can be expected.

3.4 Inverse analysis: the cost function

The cost function to be minimized during the identification procedure is the relative error between maximum forces (F_k) and strains (ε_{ijk}) obtained from numerical model (described in Section 4) adopting a given set of identification parameters $(n, \overline{\tau}, \overline{s})$, and experimental data $(\overline{F}_k, \overline{\varepsilon}_{ijk})$, i.e.:

$$H = \sum_{k=1}^{4} \left[w_1 \cdot \left(\frac{F_k - \overline{F}_k}{\overline{F}_k} \right)^2 + w_2 \cdot \sum_{i=1}^{m} \sum_{j=1}^{f} \left(\frac{\varepsilon_{ijk} - \overline{\varepsilon}_{ijk}}{\overline{\varepsilon}_{1jk}} \right)^2 \right], \tag{8}$$

where subscripts i, j, k indicate, respectively, i-th position of strain gauge along the plate ($i=1:m$), j-th level of applied load in a delamination test ($j=1:f$), and k-th bonded length BL ($k=1:4$); moreover, f and m are numbers of selected load levels and strain gauges along the plate, and w_1, w_2 are weight constants for forces and strains. Values are set in a non-

dimensional form with respect to experimental force ($\overline{F}_k$) and to strain corresponding to first strain gage ($\overline{\varepsilon}_{1jk}$), respectively.

4 MODEL FOR FRP-CONCRETE DELAMINATION

A non-linear bond – slip model has been recently developed by the authors to study FRP-concrete delamination phenomenon (Ferracuti et al. 2006). Notation adopted for displacements and stresses is reported in Figure 4. Plate and concrete are subject to axial deformation only, i.e., bending of plates is neglected. This assumption is valid in the present case, due to negligible bending stiffness of FRP plate with respect to concrete specimen counterpart.

Axial displacements and forces for concrete and plate are denoted by u_c, u_p, σ_c, σ_p. The governing equations are equilibrium, constitutive and compatibility conditions, which can be written in the form:

$$\frac{\mathrm{d}u_p}{\mathrm{d}x} = \frac{\sigma_p}{E_p}, \qquad \frac{\mathrm{d}\sigma_p}{\mathrm{d}x} = \frac{\tau}{h_p}, \tag{9}$$

$$\frac{\mathrm{d}u_c}{\mathrm{d}x} = \frac{\sigma_c}{E_c}, \qquad \frac{\mathrm{d}\sigma_c}{\mathrm{d}x} = -\frac{b_p}{A_c}\tau, \tag{10}$$

where A and E stand for area and Young modulus, respectively, and subscripts c, p for concrete and FRP plate.

According to notation reported in Figure 4, FRP – concrete interface law is then written in the form:

$$\tau_p = k_p(s_p) \cdot s_p, \tag{11}$$

where $s_p = u_p - u_c$ denotes FRP-concrete slip and $k_p(s_p)$ is the non-linear secant stiffness of interface law.

By substituting Equation 11 in Equations 9, 10, a system of non-linear first order differential equations can be obtained:

$$\frac{\mathrm{d}\mathbf{y}(x)}{\mathrm{d}x} = \mathbf{A}(\mathbf{y},x)\mathbf{y}(x), \qquad 0 \le x \le BL, \tag{12}$$

where BL is the length of the bonded plate, vector $\mathbf{y}$ collects the unknown functions:
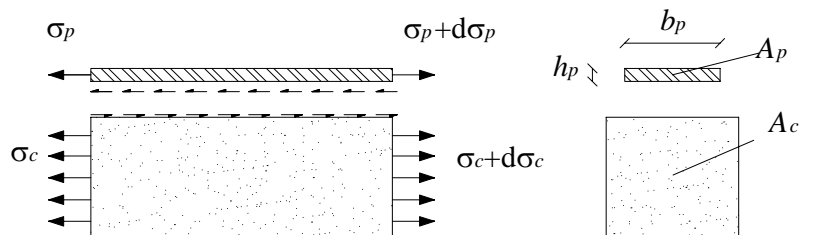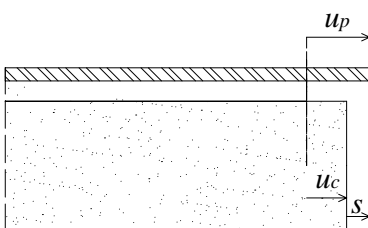
$$\mathbf{y}^T = \left\{N_p, N_c, u_p, u_c\right\} \tag{13}$$

and the non-linear matrix $\mathbf{A}$ is:

$$\mathbf{A} = \begin{bmatrix} 0 & 0 & b_p\,k_p & -b_p\,k_p \\ 0 & 0 & -b_p\,k_p & b_p\,k_p \\ 1/E_p\,A_p & 0 & 0 & 0 \\ 0 & 1/E_c\,A_c & 0 & 0 \end{bmatrix}. \tag{14}$$

5 INVERSE ANALYSIS BY DIFFERENTIAL EVOLUTION ALGORITHM

Differential Evolution (DE) is a heuristic direct search approach (Storn & Price 1997). A number NP of vectors containing the optimization parameters is adopted:

$$\mathbf{z}_{i,M} = \left\{n, \overline{\tau}, \overline{s}\right\}, \qquad i = 1,2,...,NP$$

Subscript M indicates the M-th generation of parameter vectors, called *population*. The number NP of vectors of the population is kept constant during the minimization process.

In order to minimize the objective function, a direct search method is a strategy that generates variations of parameter vectors. A robust algorithm requires that solution does not converge to a local minimum. Techniques like genetic and evolution algorithms are based on the calculation of several vectors simultaneously. Hence, if some vectors reach local minima, they can be excluded because they are associated with higher values of the cost function.

DE algorithm is briefly described. First of all, initial population is chosen randomly. Then, DE generates a new parameter vector by adding the weighted difference vector between two vectors of the population, so obtaining a third vector (*Mutation* operation). Then, in the *Crossover* operation, a new trial vector is generated by selecting some components of the mutant vector and some of the original vector. If the *trial vector* gives a lower value of objective function than that of the old population, the new generated vector replaces the old vector (*Selection* operation). These operations are described with more details in the following.

5.1 *Mutation*

For each vector of M-th population $\mathbf{z}_{i,M}$, $i= 1, 2, …,$

Figure 4. The bond-slip model for FRP-concrete delamination: notation adopted for displacements and stresses.
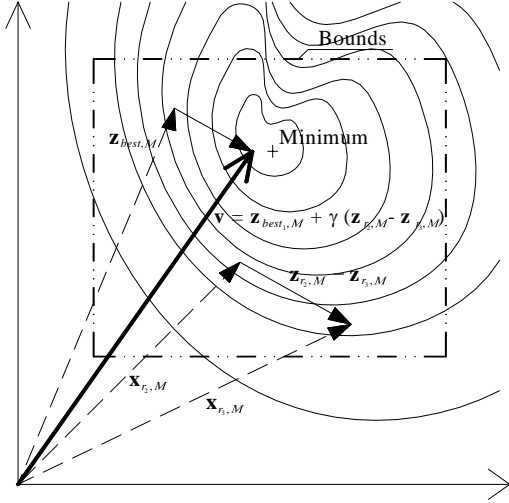
Figure 5. Differential Evolution algorithm for parameter identification: mutation operation (according to best combination).

NP, a trial vector $\mathbf{v}_{i,M}$ is generated by adding to $\mathbf{z}_{i,M}$ a contribution obtained as the difference between two other vectors of the same population.

According to Storn & Price (1997), the mutant vector is generated according to the expression:

$$\mathbf{v}_{i,M+1} = \mathbf{z}_{best,M} + \gamma \cdot (\mathbf{z}_{r_1,M} - \mathbf{z}_{r_2,M}), \qquad (15)$$

where $r_1, r_2 \in \{1,2,...,NP\}$ are mutually different integer numbers and $\mathbf{z}_{best,M}$ is the vector giving the minimum value of the object function of the M-th population (see Figure 5) Moreover, $\gamma < 2$ is a positive constant (scale parameter) controlling the amplitude of the mutation.

5.2 *Crossover*

In order to increase the diversity of the vectors, crossover process is introduced in the DE algorithm.

The *trial vector* $\mathbf{u}_{i,M+1}$ is obtained by randomly exchanging the values of optimization parameters between the original vectors of the population $\mathbf{z}_{i,M}$ and those of mutant population $\mathbf{v}_{i,M+1}$, i.e.:

$$\mathbf{u}_{i,M+1} = \{u_{1i,M+1}, u_{2i,M+1}, u_{3i,M+1}\},$$

where:

$$\left(\mathbf{u}_{i,M+1}\right)_j = \begin{cases} \left(\mathbf{v}_{i,M+1}\right)_j & \text{if } rand(j) \le CR \\ \left(\mathbf{z}_{i,M}\right)_j & \text{if } rand(j) > CR \end{cases} \qquad (16)$$

In Equation 16, $j = 1,2,3$ and $(\mathbf{u}_{i,M+1})_j$ is the j-th component of vector $\mathbf{u}_i$. Moreover, $rand(j)$ is the j-th value of a vector of uniformly distributed random numbers, and CR is the crossover constant ($0 < CR < 1$), indicating the percentage of mutations.

5.3 *Selection*

In order to decide if a vector $\mathbf{u}_i$ may be element of new population of generation $M+1$, each element of the vector $\mathbf{u}_{i,M+1}$ will be compared with the previous vector $\mathbf{z}_{i,M}$. If vector $\mathbf{u}_{i,M+1}$ gives a smaller value of objective function H than $\mathbf{z}_{i,M}$, $\mathbf{u}_{i,M+1}$ is selected as the new vector of population $M+1$.

Otherwise, the old vector $\mathbf{z}_{i,M}$ is retained, i.e.:

$$\mathbf{z}_{i,M+1} = \begin{cases} \mathbf{u}_{i,M+1} & H(\mathbf{u}_{i,M+1}) < H(\mathbf{z}_{i,M}) \\ \mathbf{z}_{i,M} & H(\mathbf{u}_{i,M+1}) \ge H(\mathbf{z}_{i,M}) \end{cases} \qquad (17)$$

with $i = 1,2,...,NP$.

6 NUMERICAL APPLICATION

Inverse analysis procedure is applied to the present problem, adopting the cost function reported in Equation 8, with weight constants for force and strain contributions equal to $w_1 = 1$ and $w_2 = 1/f$ (f being the number of load levels considered), respectively. For three unknown parameters of interface law $(n, \bar{\tau}, \bar{s})$, the values $n = 3.008$, $\bar{\tau} = 7.72$ and $\bar{s} = 0.0218$ have been obtained. In the following, the present solution will be denoted as *Case A*.

6.1 *Numerical against experimental results*

Experimental tests have been then numerically simulated with the bond-slip model described in Section 4 and identified values of parameters $(n, \bar{\tau}, \bar{s})$; results have then been compared with experimental
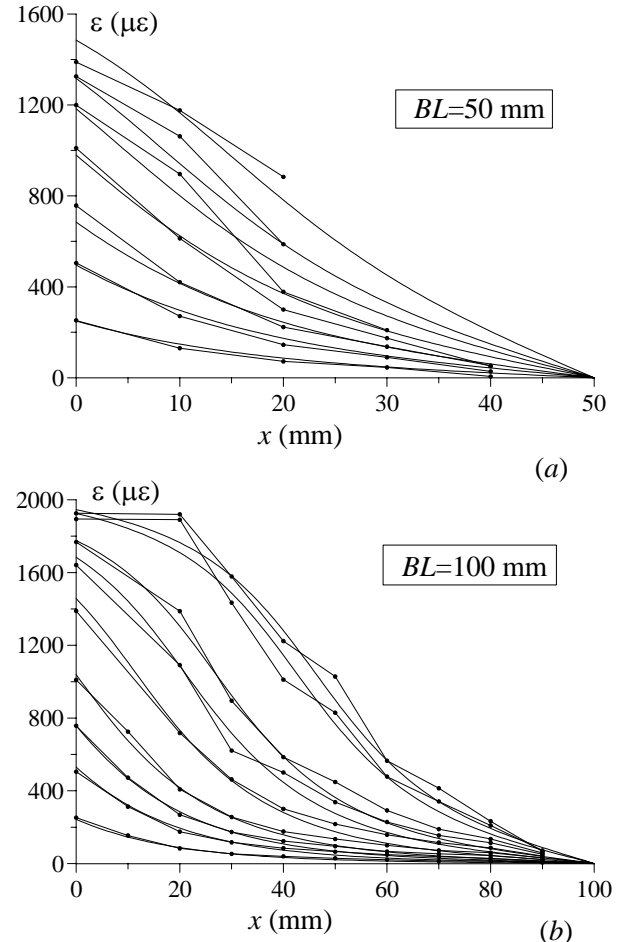

Figure 6. Strains along the bond length at different loading levels: numerical results (——) and experimental data from Mazzotti et al. (2007) (•••): *(a)* $BL = 50$ mm, *(b)* $BL = 100$ mm.

data.

Strain distributions in FRP plate along the bonded length are given in Figure 6 for 50 mm and 100 mm bond length, respectively. The highest load level considered is close to failure load obtained experimentally. Numerical results are generally in good agreement with experimental data. For all bonded lengths, the behavior for low loads is very well predicted, so assuring that stiffness of initial (elastic) branch of interface laws is correctly evaluated. Moreover, the bond-slip model is able to follow the growth of delamination at constant load along the bonded length.

FRP strain and shear stress distributions for bonded lengths equal to 200 mm and 400 mm are reported in Figures 7, 8; white dots refer to data obtained during delamination phase. As for shear

stresses, numerical and experimental results are in good agreement for low – to – medium loadings. For very high loads, i.e., when plate delamination is in progress, results obtained from experimental data are more irregular. In any case, position of maximum shear stress along the bonded length is well predicted.

Finally, delamination loads obtained numerically as a function of bonded length are compared with experimental results in Figure 9 (see *Case A*). Results confirm that the proposed interface law provides for a good prediction of failure loads. For the smallest bonded length (50 mm), the experimental load is lower than predicted numerically: when the length of the plate is smaller than width, assumption of plane deformation adopted for 1D bond-slip model is not longer valid, and a more complex non
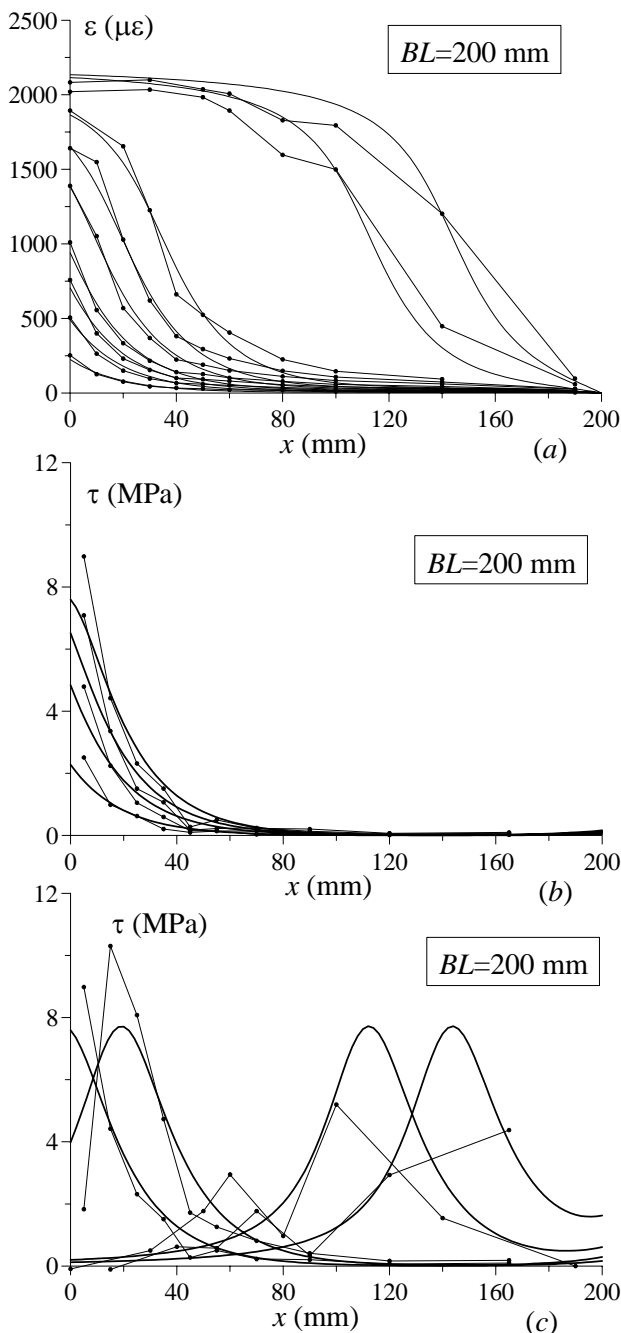

Figure 7. (*a*) Strains and (*b, c*) shear stresses at low and high loading levels: numerical results (—) and experimental data from Mazzotti et al. (2007) (•••), for *BL* = 200 mm.
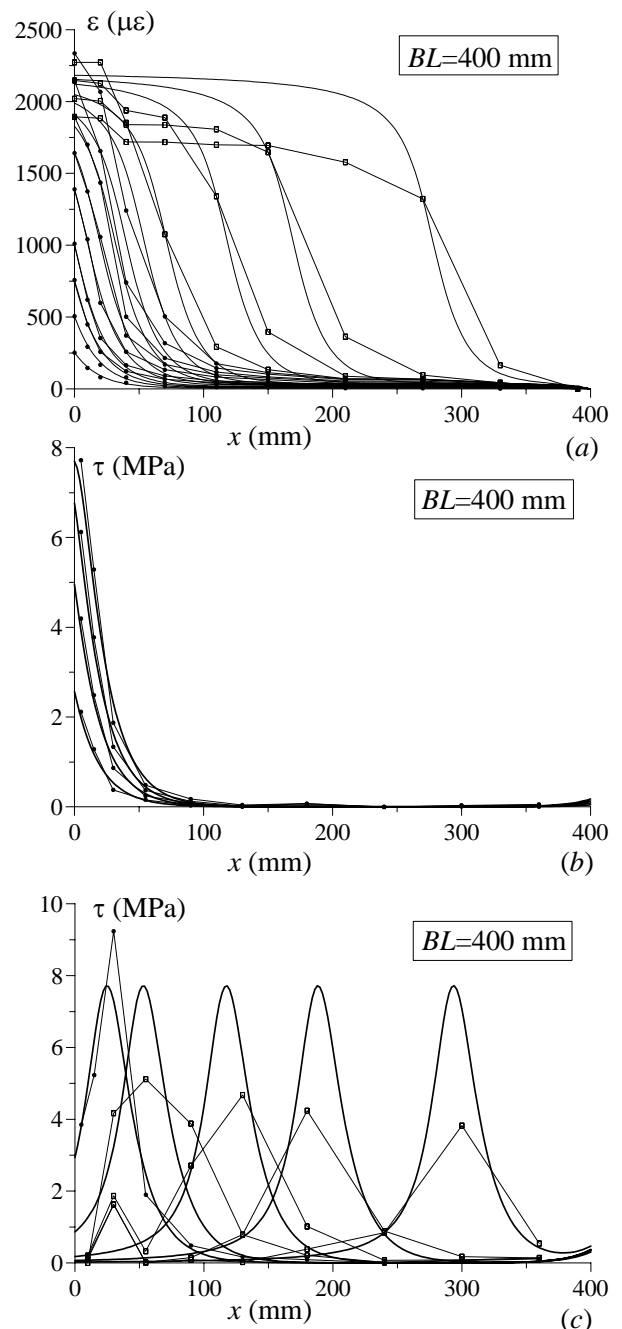
Figure 8. (*a*) Strains and (*b,c*) shear stresses at low and high loading levels: numerical results (—) and experimental data from Mazzotti et al. (2007) (•••), for *BL* = 400 mm.
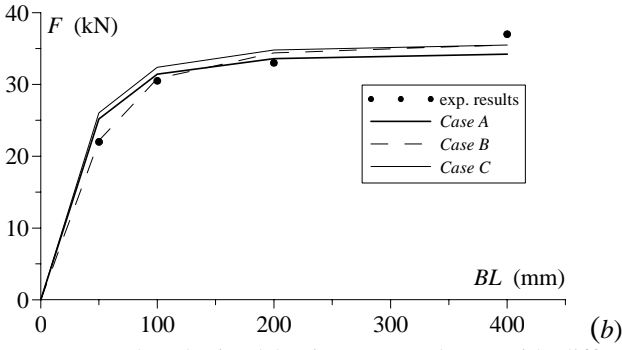
Figure 9: Results obtained by inverse analyses with different cost functions: maximum force vs bond length compared with experimental results.

linear 3D model should be required.

6.2 *Well-posedness of inverse problem*

The choice of cost function to be minimized is very important to obtain a well-posed inverse problem for parameter identification. This problem, well known in dynamic identification problems (Savoia & Vincenzi 2005), has been recently treated in Iacono et al. 2006 for parameter identification of non local damage problems.

In the present study, three different cost functions have been considered, with different values of w_1, w_2 weight constants for force and strain contributions in Equation 8.

In the first case (*Case A*), both maximum forces at delamination for different bonding lengths and FRP strains at different force levels have been adopted, with $w_1 = 1$, $w_2 = 1/f$ in Equation 8. This problem has been described in the previous section, and the corresponding solution is considered as the reference solution. In the second case (*Case B*), maximum forces for different bonding lengths only have been considered in the calibration procedure ($w_1 = 1$, $w_2 = 0$). In the third case (*Case C*), strains for different loading levels and bonding lengths only have been considered ($w_1 = 0$, $w_2 = 1/f$).

For each cost function, inverse analysis has been performed by DE algorithm. Best values of unknown parameters are reported in Table 1 and interface laws are depicted in Figure 11.

Contour lines of cost function vs. $(\bar{\tau}, \bar{s})$ parameters are shown in Figure 10, setting the value of exponent n equal to the identified value for each individual case. The minimum of the three cost functions is indicated in each figure with a cross.

Figure 10*b* clearly shows that, adopting maximum forces only (*Case B*), a direction exists where the cost function is almost insensitive to variations of identification parameters $\bar{\tau}, \bar{s}$. That direction corresponds to constant values of fracture energy of interface law (see Equation 4). For *Case C* (strain measures only), cost function is similar to reference *Case A*. However, minimum curvature is smaller, so indicating that identification of unknown parameters can be numerically more computationally expensive.
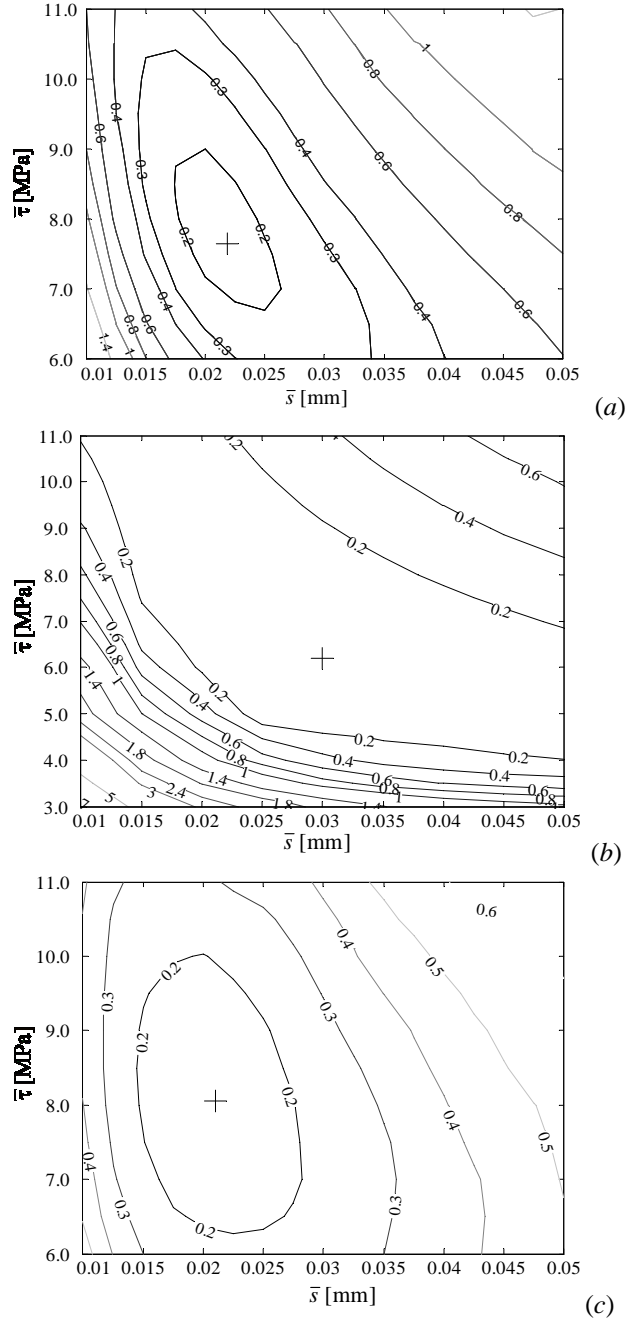

Figure 10. Cost function obtained for (*a*) *Case A* for $n = 3.00$ (reference solution), (*b*) *Case B* for $n = 3.04$, (*c*) *Case C* for $n = 2.98$.

A sensitivity analysis has been also performed to determine minimum curvature of objective functions (see Table 1). Results clearly show that, adopting both forces and strains, minimum curvature of cost function increases by a factor greater than 6 with respect to the case of only forces. Of course, smaller values indicate smaller sensitivity of cost function to parameter variation.

Finally, in Figure 11, debonding forces obtained with interface laws whose parameters have been obtained by adopting different cost functions are compared with experimental results. Smallest error in terms of debonding forces is obtained in *Case B* whose cost function is based on global data (forces) only. Nevertheless, in this case the error on strain profiles is much higher that reference Case A as shown in Figure 12.
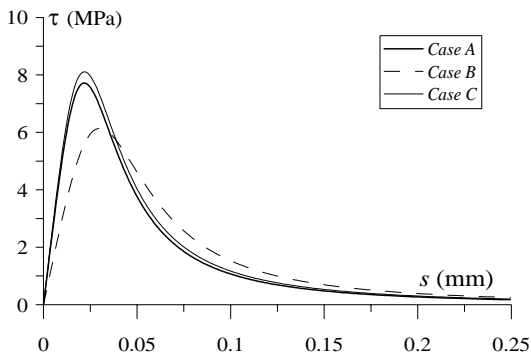
Figure 11: Results obtained by inverse analyses with different cost functions: FRP – concrete interface laws
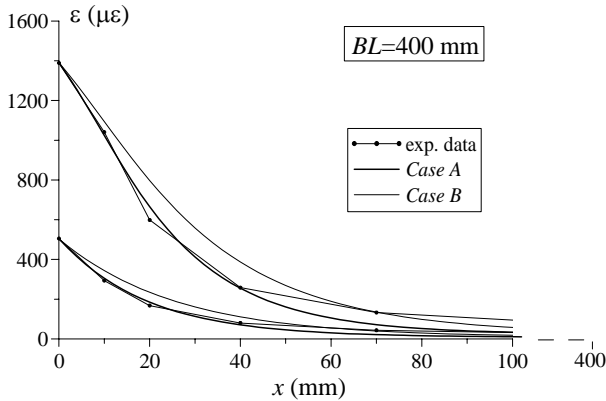

Figure 12: Results obtained by inverse analyses with different cost functions: distribution of strain along the plate.

Table 1. Comparison between results obtained by inverse analysis with different cost function.

Case	n	$\bar{\tau}$	$\bar{s}$	G_f	Min curvature
	-	MPa	mm	MPa mm	-
A	3.01	7.72	0.0218	0.4818	0.0104
B	3.04	6.14	0.0301	0.5173	0.0016
C	2.98	8.11	0.0219	0.5189	0.0098

7 CONCLUSIONS

Inverse analysis is used to derive a non linear mode II interface law for Fiber Reinforced Polymer (FRP) – concrete bonding starting from experimental data. The proposed law is based on a power fractional law depending on three parameters, maximum shear stress with corresponding slip and an exponent. Pull-pull delamination tests from Mazzotti et al. (2007) are considered: experimental data are both maximum forces and strain profiles along FRP plate. A direct search method (Differential Evolution algorithm) is used to solve the inverse problem. Well-posedness of inverse problems adopting different cost functions is discussed. It is shown that, if only maximum forces are adopted, the problem is ill-posed and cost function is much less sensitive to parameter variation. On the contrary, if both maximum forces and FRP strain are used, sensitivity of cost function to parameter variation is much higher and identification can be performed correctly.

Adopting the so obtained mode II interface law and the bond – slip model described in Section 4, very good agreement is found between numerical and experimental results, in terms of FRP strains, shear stress profiles before and during delamination and values of maximum forces, so assessing the validity of the proposed technique.

REFERENCES

Brosens, K. 2001. Anchorage of externally bonded steel plates and CFRP laminates for the strengthening of concrete elements. *Ph. D. thesis*, Univ. of Leuven, Belgium.

Chen, J.F & Teng, J.G. 2001. Anchorage strength models for FRP and steel plates bonded to concrete. *J. Struct. Eng. ASCE* 127(1): 784-91.

CNR Committee. 2006 *Guide for the design and construction of externally bonded FRP systems for strengthening existing structures,* CNR DT 200/2004 Technical Report.

Ferracuti B., Savoia M. & Mazzotti C. 2006. A numerical model for FRP–concrete delamination. *Composites Part B: Engineering*, 37 (4-5): 356-364.

Ferracuti, B., Savoia, M. & Mazzotti, C. 2007. Interface law for FRP-concrete delamination. *Composite Structures*, in press.

Iacono, C., Sluys L. J., & van Mier J. G. M.. 2006. Estimation of model parameters in nonlocal damage theories by inverse analysis techniques. *Computer Methods in Applied Mechanics and Engineering* 195: 7211–7222.

Lu, X.Z., Teng, J.G., Ye, L.P. & Jiang, J.G. 2005. Bond – slip models for FRP sheets/plates bonded to concrete. *Eng. Struct.* 27(4): 920-937.

Mazzotti, C., Savoia, M. & Ferracuti B. 2007. An Experimental study on delamination of FRP plates bonded to concrete. Submitted.

Neto, P., Alfaiate, J., Almeida, J.R., Pires, E.B. & Vinagre, J. 2004. The influence of the mode II fracture energy on the behaviour of composite plate reinforced concrete. In: Li et al., editors. *Proceedings FraMCoS-5*. Vail, Colorado. USA.

Savoia M. & Vincenzi L. 2005. Differential evolution algorithm in dynamic structural identification, *ICOSSAR - International conference of structural safety and reliability,* Rome, Italy.

Slowik, V., Villmann, B. & Bretschneider, N. 2006. Computational aspects of inverse analyses for determining softening curves of concrete. *Computer Methods in Applied Mechanics and Engineering* 195 (52): 7223-7236.

Storn, R. & Price, K. 1997. Differential Evolution - a simple and efficient heuristic for global optimization over continuous spaces. *Journal of Global Optimization* 11 (4): 341-359.

Teng, J.G. 2001. *FRP composites in civil engineering*. Hong Kong: Elsevier.

Teng, J.G., Smith & S.T. 2002. FRP-strengthened RC beams. I: review of debonding strength models. *Eng. Struct.* 24(4): 385-95.

Teng, J.G., Smith, S.T., Yao, J. & Chen, J.F. 2003. Intermediate crack-induced debonding in RC beams and slabs. *Construction and Building Materials* 17(6-7): 447-62.

Wu, Z., Yuan, H. & Niu, H. 2002. Stress transfer and fracture propagation in different kinds of adhesive joints. *J. Eng. Mech. ASCE* 128(5): 562-73.

Yuan, H., Teng, J.G., Seracino, R., Wu, Z.S. & Yao, J. 2004. Full-range behavior of FRP-to-concrete bonded joints. *Eng. Struct.* 26: 553-65.